Ocean Engineering 202 (2020) 106886

Contents lists available at ScienceDirect

Ocean Engineering

journal homepage: www.elsevier.com/locate/oceaneng

Design of an adaptive noise canceller for improving performance of an autonomous underwater vehicle-towed linear array

Cheng Chi *, Venugopalan Pallayil, Mandar Chitre

Acoustic Research Laboratory, Tropical Marine Science Institute, National University of Singapore, 18 Kent Ridge Road, 119227, Singapore

ARTICLE INFO

Keywords:
Adaptive noise canceller
Autonomous underwater vehicle
Towed linear array
Underwater sensing system for AUVs

ABSTRACT

Noise radiated from an autonomous underwater vehicle (AUV) is one of the major sources of interference that impact the acoustic performance of its towed array sensor, especially during passive detection under low ambient noise conditions. In this paper, an adaptive noise canceller (ANC) based on the partitioned fast block least-mean-square adaptive algorithm is designed and applied to mitigate the AUV-radiated noise to improve the detection performance of a linear array towed by an AUV platform. The gain, defined as the ratio of the output signal-to-noise ratio (SNR) to the input SNR, is taken as the metric for our ANC. Results obtained from processing the experimental data indicate that the gain of the ANC is up to 20 dB.

1. Introduction

The mobility and autonomy of autonomous underwater vehicles (AUVs) allow them to operate without intervention, and over larger areas, making them very attractive for underwater applications (Holmes et al., 2006; Newhall et al., 2017; Glegg et al., 2001; Ferri et al., 2018; Munafò et al., 2017; Chotiros and Pallayil, 2013). An array of hydrophones towed by AUVs is able to provide a larger aperture for directional sensing underwater, than a single hydrophone or an array of hydrophones mounted on AUVs, especially at low frequencies. AUVs fitted with towed arrays hence provide a useful tool for underwater detection and surveillance applications (Holmes et al., 2005; Pallayil et al., 2007, 2009; Maguer et al., 2008).

The radiated noise from an AUV is a major concern for towed arrays and needs to be addressed to improve the detection performance. Fig. 1 shows the spectrogram of data collected by using an AUV-towed array system during one of our experiments with and without the AUV in motion. It can be found that there is significant AUV noise could potentially mask detection of some of the underwater objects of interest. There are other studies conducted on the characteristics of noise radiated from AUVs, leading to similar conclusions that it could reduce the passive detection capabilities of towed arrays, especially under low ambient noise conditions (Munafò et al., 2017; Cheng and Pallayil, 2017; Holmes et al., 2010; Zimmerman et al., 2005; Griffiths et al., 2001). It is therefore necessary to mitigate the effect of AUV noise on the array to improve its detection performance.

Many researchers have investigated the effect of ship-radiated noise on conventional large towed arrays and how to reduce their impact on array performance (Candy and Sullivan, 2005; Sullivan and Candy, 2005). Most studies provide only a theoretical framework, and are based on reference signals. They have also not discussed how to choose the reference signals for their proposed methods. In reference Cederholm and Jönsson (2008), results from processing of real data are given, but their methods require prior knowledge of ship noise, which may be difficult to obtain in many cases. The characteristic of AUV-radiated noise is however different from that of ship-radiated noise, as AUVs employ electrical motors. For their propulsion system, the speed of an AUV is generally low, which means that cavitation noise is not very significant, when compared with ship noise (Arveson and Vendittis, 2000; Hodges, 2011). From references Munafò et al. (2017), Holmes et al. (2010), Zimmerman et al. (2005), and Griffiths et al. (2001), it can be found that the noise sources of AUV under study are dominated by the acoustic noise due to AUV vibration. The noise spectrum of AUV mainly consists of a few strong narrowband components, and the frequency range is higher than that of ship-radiated noise (Arveson and Vendittis, 2000; Holmes et al., 2010; Zimmerman et al., 2005; Hodges, 2011). Therefore, suppressing AUV-radiated noise at the towed array sensors may require a modified approach, different from the existing techniques applied to ship-based towed arrays.

There is limited information available in open literature on how to design an adaptive noise canceller (ANC) for AUV-towed array systems. We address the gap by proposing an ANC and evaluate its performance

* Corresponding author.
E-mail address: chicheng@mail.ioa.ac.cn (C. Chi).

https://doi.org/10.1016/j.oceaneng.2019.106886
Received 28 November 2018; Received in revised form 15 November 2019; Accepted 23 December 2019
Available online 6 March 2020

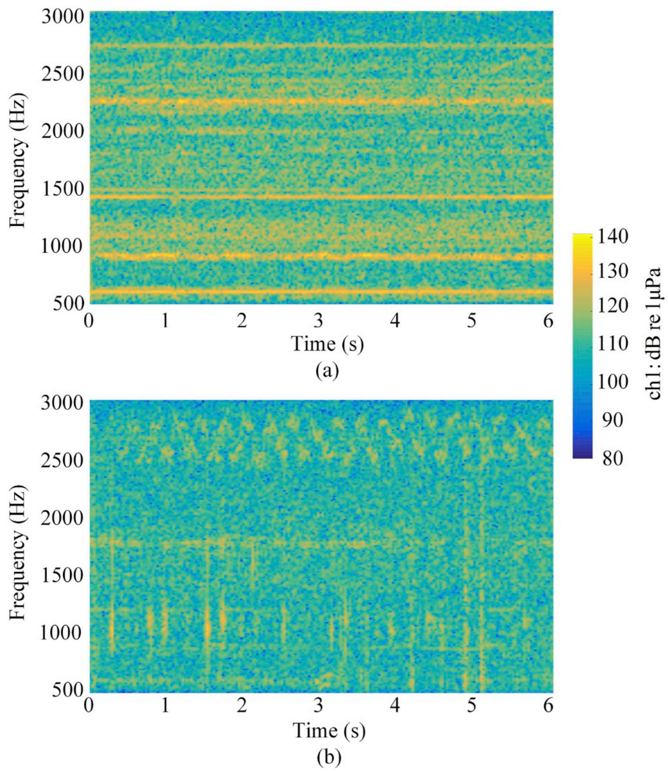

Fig. 1. Spectrogram of the signal received by the first channel of AUV-towed array. (a) When the AUV was moving steadily at a speed of 3 knots; (b) When the AUV propulsion system was turned off.

by applying to the data collected using an AUV-towed array system. The ANC is realized by employing an adaptive filter (Widrow et al., 1975; Harrison et al., 1986; Farhang-Boroujeny, 2013; Haykin, 2002). To design the ANC, we need to determine a reference signal, filter length and an adaptive algorithm. The filter length is the number of taps used in the adaptive filter. Due to the complexity of the noise propagation from AUVs to towed arrays, the required filter length tends to be large, as will be explained in the next section. Considering both the AUV-noise spectral characteristics and the large filter length needed, the partitioned fast block least-mean-square (PFBLMS) algorithm (Farhang-Boroujeny, 2013) is employed in the designed ANC.

The gain of the ANC, defined as the ratio of the output signal-to-noise ratio (SNR) to input SNR of the ANC is used to evaluate the performance (Widrow et al., 1975). The noise in the definition of the gain refers to the AUV noise received. The results of processing data from the array show that the gain of the ANC designed is up to 20 dB. We also evaluate the performance of the ANC through beamforming the array output and by injecting a source which is embedded below the interfering signal. The results show that a source 20 dB below the interfering signal could be successfully detected by using the ANC.

The contributions of this paper can be summarized as follows:

- extending the technique of adaptive noise cancellation into a new application, mitigating AUV noise on its towed array system;
- designing a special and promising ANC with considering the characteristics of the AUV noise received at the array.

This paper is organized as follows. Section 2 discusses the characteristics of AUV noise received at towed arrays. The ANC design is presented in Section 3. Section 4 evaluates the performance and computational complexity of the designed ANC. The outcomes of the study are concluded in Section 5.

2. Characteristics of the AUV radiated noise

Before designing an ANC, it is necessary to figure out the characteristics of the AUV noise received at our towed linear array. We analyze the characteristics of the noise spectrum, its propagation, and autocorrelation time in this section.

2.1. Spectrum of the received noise

The spectral characteristic of the AUV noise is an important consideration, when choosing or designing an adaptive algorithm for the ANC. Fig. 1 shows that the spectrum of the AUV noise consists of several strong narrowband components. For comparison, the spectrogram of the data received by the array when the AUV propulsion is switched off, is also provided in the same figure. From Fig. 1, it can be observed that the noise level received at the array drops substantially when the AUV propulsion is switched off, indicating that the dominant noise contribution is from the AUV propulsion system.

A schematic of the experimental arrangement used for our data collection is shown in Fig. 2. The platform employed in the experiment was a mid-sized AUV of 2.50 m long, 0.32 m in diameter and weighing 150 kg. The AUV was moving at a speed of approximately 3 knots. The array has 12 acoustic channels, uniformly distributed with a channel spacing of 0.51 m.

2.2. Noise propagation from the AUV to the array

It is reasonable to assume that the majority of the AUV noise sources are nearly omni-directional (Holmes et al., 2010). The noise propagation from AUVs to towed arrays can be thought of as a complex near-field problem, limited by the bottom and surface of the ocean (Kuperman et al., 1985). The characteristics of the bottom and surface will influence noise propagation. The simple multipath model cannot describe noise propagation accurately. The complexity must be considered when determining the filter length of the ANC.

2.3. Autocorrelation time

The autocorrelation function of one segment of the AUV noise (from 500 Hz to 3000 Hz) is shown in Fig. 3. The reason we choose the frequency band from 500 Hz to 3000 Hz is that most of the power from the AUV generated noise in our experiment is distributed in this band. It is also the band of interest in the passive detection using the AUV towed array. When the correlation coefficient between two samples, namely the autocorrelation function value is low enough, the two samples are thought as uncorrelated. From Fig. 3, it can be found that the correlation coefficient decreases from 1 to 0.1. It is hence thought as in this paper that the two samples which have the correlation coefficient of 0.1 are uncorrelated. The autocorrelation time of the AUV noise received is referred to as the minimum delay between the two uncorrelated samples. From the autocorrelation function of the AUV noise in Fig. 3, we

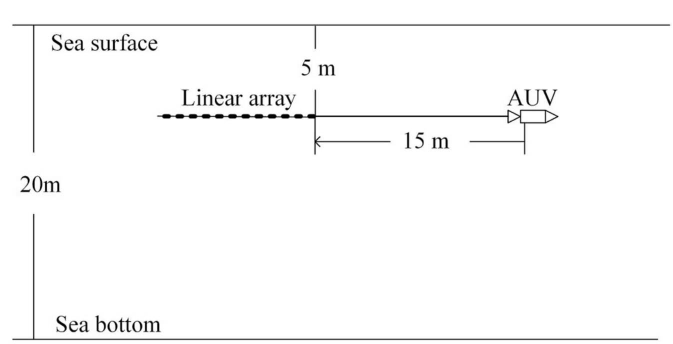

Fig. 2. Schematic of the experimental arrangement of AUV-towed array.

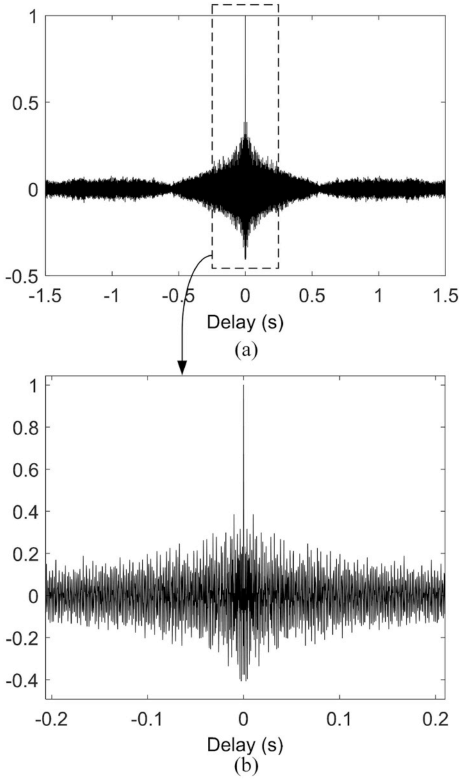

Fig. 3. Autocorrelation function of the AUV noise received by the first sensor of the array. (a) the whole view; (b) the zoom-in view of (a).

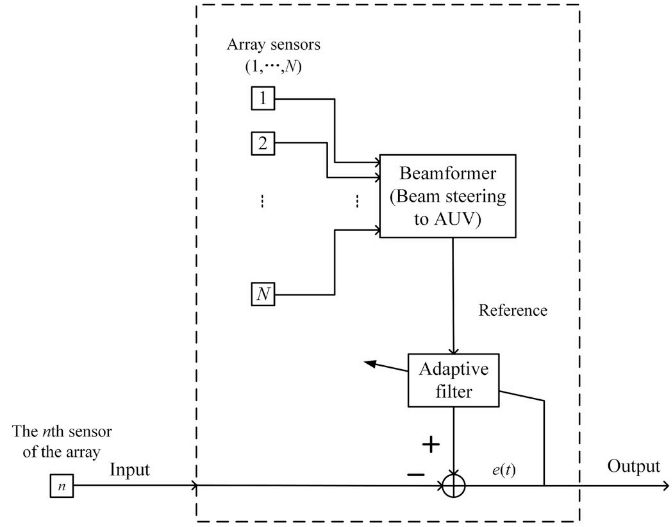

Fig. 4. The schematic of our adaptive noise canceller (ANC) for the AUV-towed linear array. The ANC takes the beamformer output with its beam steered to the AUV, as the reference signal. The input of the ANC is the signal received by the sensors of the array. The partitioned fast block least-mean-square algorithm (Farhang-Boroujeny, 2013) is used in the ANC.

obtain that the minimum delay is 0.20 s. Thus, the autocorrelation time of the AUV noise received is 0.20 s.

The autocorrelation time of the AUV noise received at the towed array can be taken as a reference to determine the adaptive filter length. For a sampling frequency of 10 kHz, based on the autocorrelation time 0.20 s, the adaptive filter length in our ANC should be larger than or equal to $0.20 \times 10{,}000 = 2000$. This large adaptive filter length poses a computational load problem in real-time noise cancellation, when using the time-domain adaptive algorithms. This problem is resolved by employing the frequency-domain adaptive algorithm based on the fast Fourier transform (FFT).

3. Design of ANC

The schematic of the designed ANC is shown in Fig. 4. As stated previously, to design an ANC for AUV-based towed array systems, we need to determine the reference signal, the adaptive filter length and the corresponding adaptive algorithm.

3.1. Reference signal

Usually, an additional sensor is placed next to the AUV for generating the reference signal. However, the additional sensor does not only increase the hardware complexity, but also potentially introduces its own noise sources which are uncorrelated to the AUV noise received by the sensors of the array, thereby impacting the performance of the ANC. Besides, the additional sensor increases the power consumption and hardware cost. In our approach, we choose the array beamformer output along the AUV direction as the reference.

It is reasonable to assume that the AUV and the towed array are lying in a straight line. This assumption has further verified by comparing the depth and heading of the array and AUV using engineering sensors, available inside the array and also on the AUV. For a uniformly weighted line array with 12 elements, the width (3 dB) of the end-fire beam is around 25° (from 65° to 90°, when using the angle definition in Fig. 6). If we steer the array beam to the AUV and weak signals which interest the AUV-towed array are not from the direction of the end-fire beam, the conventional beamforming output will amplify the AUV noise by approximately N times (Van Trees, 2004), compared to the AUV noise received at each sensor of the array. Because they are not from the direction of the AUV noise, the weak signals will not be amplified. The above analysis reveals that when using the end-fire beamformer output as the reference of the proposed ANC, if the weak signals are from the direction of the end-fire beam, the proposed ANC may not work. The blind directions of the proposed ANC will be analyzed in detail in Section 4. Every sensor of the array has a designed noise canceller. After cancelling the AUV noise received by all the sensors, the performance of the array will be improved significantly.

3.2. Adaptive filter length

Although the noise propagation from the AUV to the towed array is complex, the propagation delays calculated based on the geometry of the surface and bottom can still be taken as a reference for estimating the adaptive filter length. When calculating the delay, the simple multipath model is assumed. We only considered the paths reflected by the bottom or surface. As shown in Fig. 5, d is the distance between the AUV and first sensor of the array, l is the length of the array, h_1 is the ocean depth, and h_2 is the operating depth of the array. When $h_2 < h_1/2$, the delay for determining the adaptive filter length can be determined by the

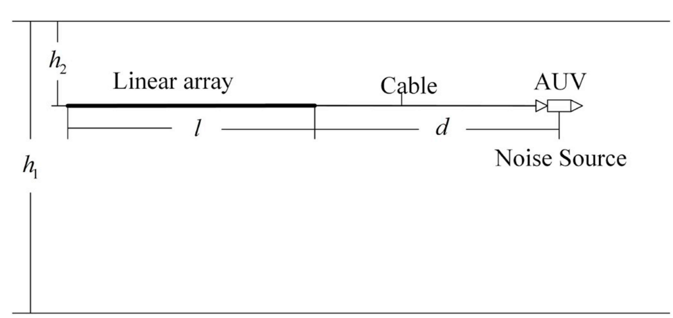

Fig. 5. Geometry of AUV towing a linear array in a shallow-water environment.

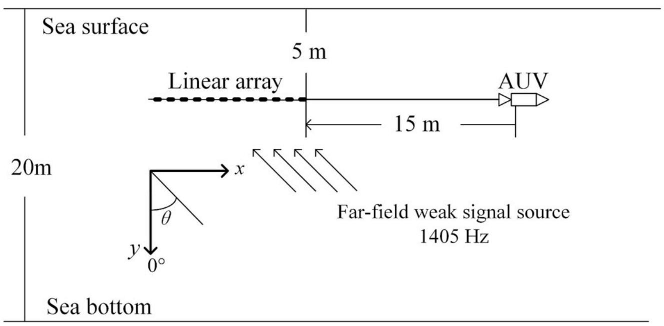

Fig. 6. Schematic of the operational considered for applying the ANC.

propagation delay corresponding to the path reflected via the bottom. Similarly, when $h_2 > h_1/2$, the delay for determining the adaptive filter length is determined by the propagation delay related to the path reflected via the surface. The propagation delay due to the bottom reflected path can be calculated by the following formula:

$$\tau_0 = \frac{2\sqrt{\left[\left(\frac{l+d}{2}\right)^2 + (h_1 - h_2)^2\right]}}{c}, \tag{1}$$

where c is the sound speed. Let f_s denote the sampling frequency. If we use the delay to estimate the adaptive filter length required, it can be expressed as

$$N = \lfloor f_s \tau_0 \rfloor, \tag{2}$$

where '$\lfloor . \rfloor$' represents the operation of obtaining the minimum integer, larger than or equal to $f_s\tau_0$.

The ANC is designed to be robust to the shallow-water environment, as one would expect large delays due to multiple reflections at the ocean boundaries. For illustration, we choose a typical shallow-water environment, with parameters are as follows: $h_1 = 80$ m, $h_2 = 10$ m, $d = 15$ m, $l = 6$ m, $c = 1500$ m/s, and $f_s = 10$ kHz. According to Eqs. (1) and (2), $N = 944$. In a more practical case, more paths reflected by the bottom and surface may arrive at the towed array. Further, the propagation of the AUV noise from the AUV to the array is a near-field problem, which is more complex than the multipath model. Therefore, when designing the ANC, which is robust to the shallow-water environment, the adaptive filter length should be much larger than 944.

The above multipath analysis of using the propagation delays shows that the adaptive filter length should be larger than 944. Based on the analysis of the autocorrelation time in Section 2.3, to make sure that all the correlated samples can be canceled, the adaptive filter duration should longer than the autocorrelation time of 0.20 s, which means the adaptive filter length required should be larger than 2000 (0.20 × 10,000), with the sampling frequency of 10,000 Hz. In our adaptive algorithm shown in the following section, FFT is used, which requires the adaptive filter length to be a power of two. Hence, we have chosen an adaptive filter length of 2048 in our design.

3.3. Adaptive algorithm

Having determined the reference signal and adaptive filter length, we need to choose what kind of adaptive algorithms to be used, based on the noise characteristics and the filter length. Two factors that we have considered in the choice of adaptive algorithm are fast convergence behavior and efficient implementation.

The large adaptive filter length increases the computational load, leading to slow convergence when using the time-domain least-mean-square (LMS) adaptive algorithm. The fast block realization of the frequency-domain adaptive algorithm (Farhang-Boroujeny, 2013) will reduce the computational load and is therefore used in this study.

The convergence behavior of the time-domain LMS adaptive algorithms is generally determined by the eigenvalues of the correlation matrix $\mathbf{R}$. The correlation matrix is defined as

$$\mathbf{R} = \mathrm{E}\left[\mathbf{x}(n)\mathbf{x}^{\mathrm{H}}(n)\right], \tag{3}$$

where $\mathrm{E}[\cdot]$ denotes statistical expectation, the superscript H denotes Hermitian transpose, and $\mathbf{x}(n)$ is an observation vector of a wide-sense stationary stochastic process $\{x(n)\}$ of an adaptive filter input. $\mathbf{R}$ can be estimated by using time average. The eigenvalues of $\mathbf{R}$ are directly related to the power spectral density (PSD) of the adaptive filter input process (Farhang-Boroujeny, 2013). The PSD reflects the spectral content of the underlying process as a function of frequency. The PSD can be estimated by using the discrete Fourier transform of the obtained correlation function of $\{x(n)\}$. The convergence behavior of the time-domain LMS algorithm is frequency dependent. Assume the transfer function of an adaptive filter is $W(e^{j\omega})$. The rate of convergence of $W(e^{j\omega})$ towards its optimum value $W_o(e^{j\omega})$, at a frequency $\omega = \omega_0$, is determined by the relative value of the PSD of the input signal at $\omega = \omega_0$. A large value of the PSD (relative to the values in other frequencies) means that the adaptive filter is well excited at $\omega = \omega_0$. This results in fast convergence around $\omega = \omega_0$. The time-domain LMS adaptive algorithm converges slowly over those frequencies in which the values of the PSD are low. As mentioned in Section 2, the PSD of AUV-radiated noise consists of several narrowband components. If the time-domain LMS adaptive algorithm is used to cancel the AUV noise, the relatively small values in most of the frequencies of the AUV noise will result in slow convergence of the algorithm.

When the adaptive algorithm is realized in the frequency domain, the step-normalization adaptation operation can be employed to normalize the input PSD at all frequencies, which means the corresponding PSD values after normalization will become consistent. Then we use the normalized frequency-domain signal for the adaptation of the filter tap weights. In this situation, the convergence speed of adaptive algorithm will increase greatly according to the analysis of the previous paragraph. Therefore, considering that the PSD of AUV-radiated noise consists of several narrowband components mainly, the frequency-domain step-normalization adaptation will be a good choice.

The fast block least-mean-square (FBLMS) algorithm realizes the step adaptation in the frequency domain and includes the operation of the step-normalization adaptation (Farhang-Boroujeny, 2013; Haykin, 2002). Hence, for our application, the FBLMS algorithm is a good choice in terms of convergence speed. In fact, we choose the partitioned FBLMS algorithm, namely the PFBLMS algorithm as it is highly efficient and well suited for implementing large adaptive filters (Farhang-Boroujeny, 2013).

The FBLMS algorithm makes use of the FFT and inverse FFT (IFFT) to improve the efficiency of the adaptive filter (Farhang-Boroujeny, 2013). The efficiency of the FBLMS algorithm is high, when the block length is comparable to the adaptive filter length. However, in our application, the adaptive filter length is large, and selecting an equivalent block length translates to high delay, which cannot satisfy real-time requirements. The block adaptation in the FBLMS algorithm incorporates the estimate of the correlation matrix (related to the gradient vector of the adaptive filter) (Haykin, 2002). In practice, AUV-radiated noise received by the array is non-stationary. Thus, if the block is too long, estimation of the correlation matrix will not be accurate, leading to poor performance of the FBLMS algorithm. Therefore, for our application, block length should be much shorter than the adaptive filter length, and this is where the PFBLMS algorithm demonstrates its efficiency over the FBLMS algorithm. In our design, the adaptive filter length is 2048 and the block length is 128. If the block length becomes longer, we find that the performance of the adaptive algorithm will start to deteriorate. For these reasons, we employed the PFBLMS algorithm (Farhang-Boroujeny, 2013).

A brief description of the PFBLMS algorithm (Farhang-Boroujeny,

2013) is given here. Let $s(n)$ denote a signal received at the towed array. The strong AUV noise received at one of the sensors of the array is denoted by $v_0(n)$, where n is the sample number. Then, the received signal $x(n)$ can be expressed as

$$x(n) = s(n) + v_0(n). \tag{4}$$

The adaptive filter length is denoted by N. For the PFBLMS algorithm, N is expressed as

$$N = P{\cdot}M, \tag{5}$$

where P is the number of partitions, and M is the partition length. Let L denote the block length in the PFBLMS algorithm. M is expressed as

$$M = pL, \tag{6}$$

where p is an integer. Letter k denotes block index. The input vector of the adaptive filter (Farhang-Boroujeny, 2013) is

$$\begin{aligned}\tilde{\mathbf{x}}_0(k) = [x(kL-M)\ \ x(kL-M+1)\ \ \ldots\ \ x(kL+L-1)].\\ (k = 1, 2, \ldots, (P-1)p)\end{aligned} \tag{7}$$

The frequency-domain vector of $\tilde{\mathbf{x}}_0(k)$ is

$$\mathbf{x}_{F,0}(k) = \mathrm{FFT}(\tilde{\mathbf{x}}_0(k)), \tag{8}$$

where 'FFT()' means the fast Fourier transform operation. The output vector of the adaptive filter is

$$\mathbf{y}(k) = \text{the last } L \text{ elements of IFFT}\left(\sum_{l=0}^{P-1} \mathbf{w}_{F,l}(k) \otimes \mathbf{x}_{F,l}(k-pl)\right), \tag{9}$$

where 'IFFT()' means the operation of the inverse fast Fourier transform, '$\otimes$' denotes element-by-element multiplication of vectors, $\mathbf{w}_{F,l}(k)$ is the tap weight vector. The update of the tap weight vector is given as

$$\mathbf{w}_{F,l}(k+1) = \mathbf{w}_{F,l}(k) + 2\boldsymbol{\mu}(k) \otimes \mathbf{x}^*_{F,l}(k-pl) \otimes \mathbf{e}_F(k), \tag{10}$$

where $\boldsymbol{\mu}(k)$ is the step size vector, obtained by the step normalization, and $\mathbf{e}_F(k)$ is the frequency-domain error estimate, given as

$$\mathbf{e}_F(k) = \mathrm{FFT}\left(\begin{bmatrix}\mathbf{0}\\ \mathbf{e}(k)\end{bmatrix}\right), \tag{11}$$

where $\mathbf{e}(k)$ is the time-domain error, given as

$$\mathbf{e}(k) = \mathbf{d}(k) - \mathbf{y}(k), \tag{12}$$

where $\mathbf{d}(k)$ is the desired output vector. $\boldsymbol{\mu}(k)$ is expressed as

$$\boldsymbol{\mu}(k) = [\mu_0(k)\ \ \mu_1(k)\ \ \ldots\ \ \mu_{M'-1}(k)]^T, \tag{13}$$

where $M' = M + L$. The step normalization of the PFBLMS algorithm is given as

$$\mu_i(k) = \frac{\mu_0}{\hat{\sigma}^2_{F,0,i}(k)},\quad (i = 0\ \ldots M'-1), \tag{14}$$

where μ_0 is a common unnormalized, $\hat{\sigma}^2_{F,0,i}(k)$s are the power estimates of the samples of the filter frequency-domain input $\mathbf{x}_{F,0}(k)$, expressed as

$$\hat{\sigma}^2_{F,0,i}(k) = \beta\hat{\sigma}^2_{F,0,i}(k-1) + (1-\beta)\left|x_{F,0,i}(k)\right|^2, \tag{15}$$

where β is a constant close to, but smaller than 1. The frequency-domain step normalization is the key to the proposed ANC. The detailed steps of the PFBLMS algorithm are shown in the Appendix.

4. Performance evaluation

The performance of our designed ANC in cancelling the AUV noise, and its computational complexity are given in this section.

4.1. AUV noise cancellation performance

The designed ANC, was applied to the data collected from a sea trial. Fig. 6 shows the operational scenario during the AUV noise data collection and the injected signal. The ocean depth was 20 m. The depth of AUV was 5 m. The AUV speed was approximately 3 knots. The distance between the AUV and first sensor of the array was 15 m. The 12 hydrophone channels of the array were uniformly distributed with a channel spacing of 0.5 m, corresponding to halfwavelength at 1.5 kHz. To test the functionality of the algorithm in detecting the object signal under the AUV nosie, a weak signal was numerically added into the collected noise data. The power ratio of the weak signal to the AUV noise received by the first sensor of the array was set to −20 dB. Two frequencies of the weak signals with the same amplitude: 1300 Hz and 1405 Hz were used in our evaluation.The frequency of 1405 Hz was in one of the prominent AUV noise bands. The frequency of 1300 Hz was not overlapped with the AUV noise bands. Using the geometry definition in Fig. 6, the direction of the weak signal varied from 0° to 90°, to evaluate the ANC performance for signals from different directions.

The adaptive technique: inverse beamforming, has been successfully applied to cancel ship noise for towed line arrays (Li, 2012; Robert and Beerens, 2002). Even though the inverse beamforming method has not been applied to cancel noise for AUV-based towed array systems, we chose it as the reference method to verify our ANC. The reference method assumes that interferences or noise received at each sensor are the same except for the differences of propagation delays. The steps of the reference method are briefly given as follows:

1) Do conventional beamforming in all the directions and find the beam with the maximum magnitude;
2) Attenuate the maximum beam output by N times for the array with N sensors, and delay the attenuated beam output with different delays for different sensors;
3) Substract the signal received at each sensor by the corresponding delayed and attenuated beam output;
4) Repeat steps 1)-3), until that the weak signal is found.

The gain of a noise canceller was used as a parameter for evaluating the performance of the ANC (Widrow et al., 1975). This parameter is explained in Fig. 7 and written as

$$G = \frac{SNR_{out}}{SNR_{in}} \tag{16}$$

where SNR_{in} is the input signal-to-noise ratio (SNR) of the noise canceller, and SNR_{out} is the output SNR. Here, it should emphasized that the signal is from the far-field weak target, and the noise is the AUV-radiated noise received at the sensors of the array, which dominates the received noise and hence is required to be cancelled.

First, we evaluate the performance of the proposed ANC at different frequencies (1300 Hz and 1405 Hz), where the direction of the weak signal is 50°. Fig. 8 (a) and (b) show the PSDs of data without and with the ANC for the two frequencies used. Ideally, the weak signal should not be influenced by use of the ANC to cancel the AUV noise. From Fig. 8 (a), it can be found that when the frequency of the weak signal is not overlapped with the AUV noise band, the ANC has no observable influence on the weak signal. While Fig. 8 (b) shows that when frequency

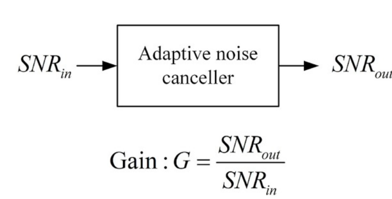

Fig. 7. Definition of the gain for evaluating the performance of adaptive noise canceller.

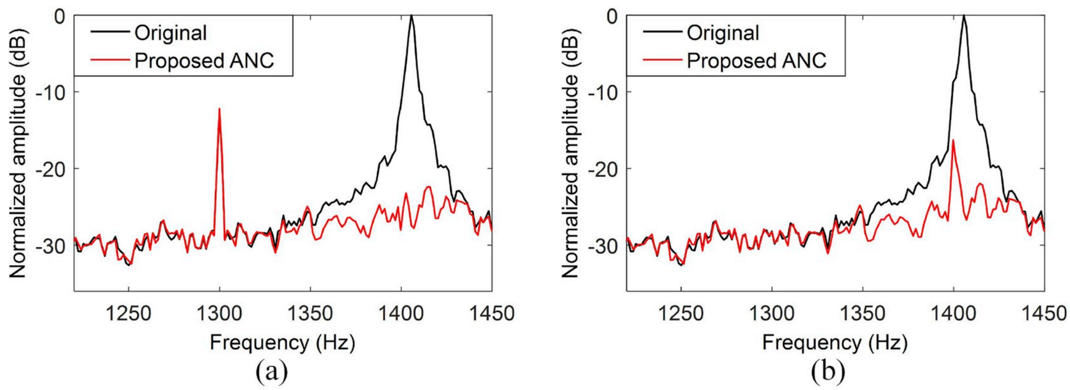

Fig. 8. Results of processing sensor 1 of our array with different signal frequencies: (a) 1300 Hz and (b) 1405 Hz, showing performance of the proposed adaptive noise canceller (ANC).

of the weak signal is overlapped with the AUV noise band, the component of the weak signal is slightly decreased. This means the situation that the signal frequency is in the frequency band of the AUV noise is more challenging for the proposed ANC. To better verify the ANC, the frequency of 1405 Hz of the weak signal is used in the following evaluation.

Data from the sea trial showed that the amplitudes of the AUV noise received at different sensors are different. Because the ANC should be robust to the sensor location, it is necessary to illustrate the processing results of different sensors. We picked up two sensor locations where the expected levels of AUV noise is maximum (sensor 1 and sensor 12). Fig. 9 (a) shows the PSDs of data from the first sensor of the array without and with the designed ANC. Fig. 10 (a) shows similar PSDs curves for the 12th sensor of the array. For comparison, the results from the reference method (the inverse beamforming (Li, 2012; Robert and Beerens, 2002)) are also provided in Figs. 9 (c) and Fig. 10 (c). It can be seen that with the ANC, the AUV noise is cancelled well and the weak signal is well identified. The performance of the reference method is not as good as that of the ANC. The reference method is based on the assumption that the AUV noise received at different sensors is the same except for the different propagation delays. The ANC in this paper has no such an assumption. The received AUV noise differs for different sensors, which is the main reason that the reference method cannot perform as good as the proposed ANC. The comparison between Figs. 9 and 10 demonstrates that the designed ANC performs well for different sensors and is robust to the noise levels at different sensors. The gain of the ANC in the frequency band around 1400 Hz, is 20 dB.

Next, we evaluate the performance of the ANC for different signal

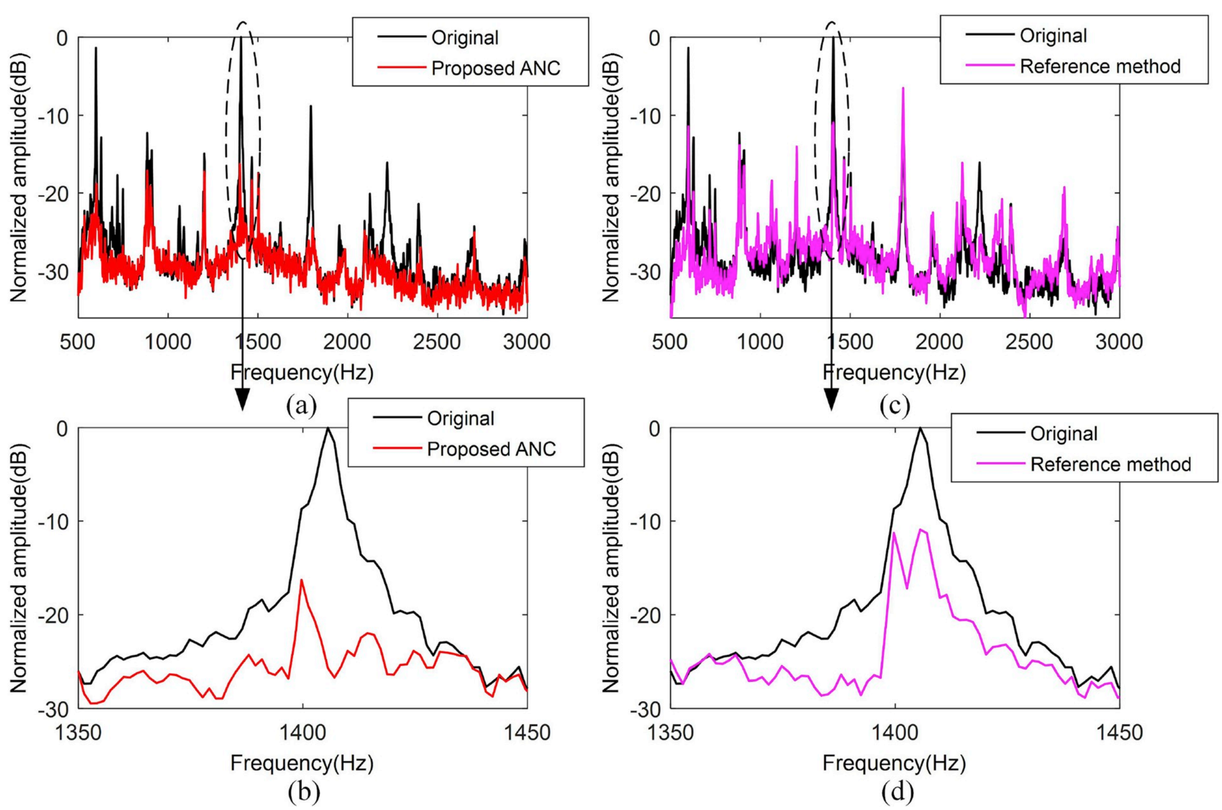

Fig. 9. Results of processing sensor 1 of our array, showing performance of the proposed adaptive noise canceller (ANC) and the reference method. (a) Power spectral densities (PSDs) of the original signal of sensor 1 and that using the proposed ANC; (b) zoomed-in view of (a) around the weak signal frequency; (c) Power spectral densities of using the reference method; (d) zoomed-in view of (c) around the weak signal frequency. (The weak signal frequency is 1405 Hz. Black curve represents the PSD of the original signal (AUV noise + added weak signal), Red curve represents the PSD afterr applying the proposed ANC and Magenta curve represents the PSD after applying the reference method.). (For interpretation of the references to colour in this figure legend, the reader is referred to the Web version of this article.)

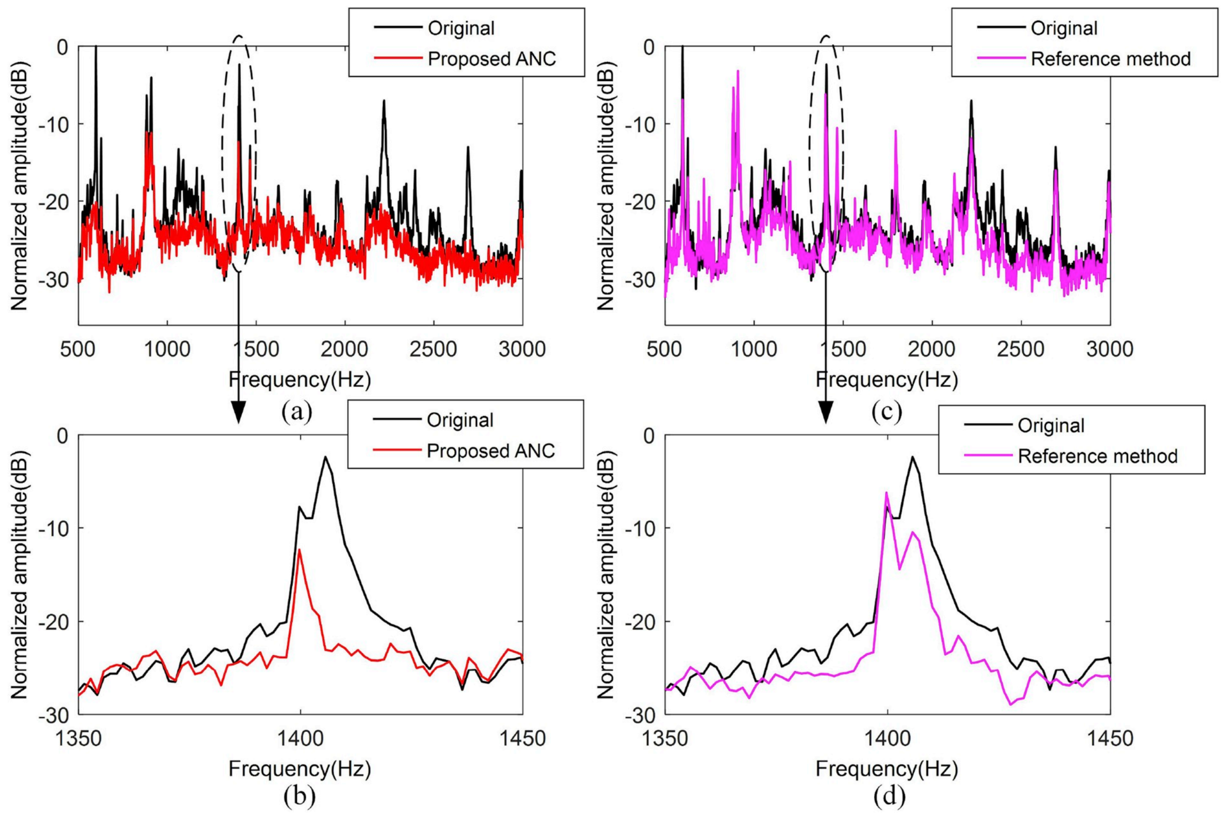

Fig. 10. Results of processing sensor 12 of our array, showing performance of the proposed adaptive noise canceller (ANC) and the reference method. (a) Power spectral densities (PSDs) of the original signal of sensor 12 and that using the proposed ANC; (b) zoomed-in view of (a) around the weak signal frequency; (c) Power spectral densities of using the reference method; (d) zoomed-in view of (c) around the weak signal frequency. (The weak signal frequency is 1405 Hz. Black curve represents the PSD of the original signal (AUV noise + added weak signal), Red curve represents the PSD after applying the proposed ANC and Magenta curve represents the PSD after applying the reference method.). (For interpretation of the references to colour in this figure legend, the reader is referred to the Web version of this article.)

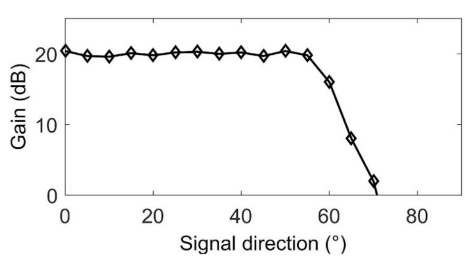

Fig. 11. The gain of the proposed ANC versus different signal directions.

directions. Fig. 11 shows the gain of the ANC from the broadside (0°) to the endfire (90°). It can be found that the performance of the ANC deteriorates for the signal direction of 60° onwards. When using the proposed ANC, this shortcoming should be noted.

Finally, the beamformed outputs of the array before and after noise cancellation are given in Fig. 12. The conventional delay-and-sum method in the time domain was used to do beamforming. From Fig. 12, it can be seen that because the AUV noise is strong, the beamformed output is not able to resolve the signal added at the relevant look direction. After using the ANC, the signal is recovered reasonably well, at the expected look angle of 50°. The arrival at broadside can be found from Fig. 12. It is caused by the electronic noise component in each sensor coupled from the same circuit. Because there is no delay among the electronic noise components of all the sensors, with beamforming, the electronic noise component is enhanced at broadside and the broadside arrival appears in Fig. 12. The problem of the electronic noise can be solved by designing a better circuit, and is not the focus of our research. This does not influence the performance evaluation of the

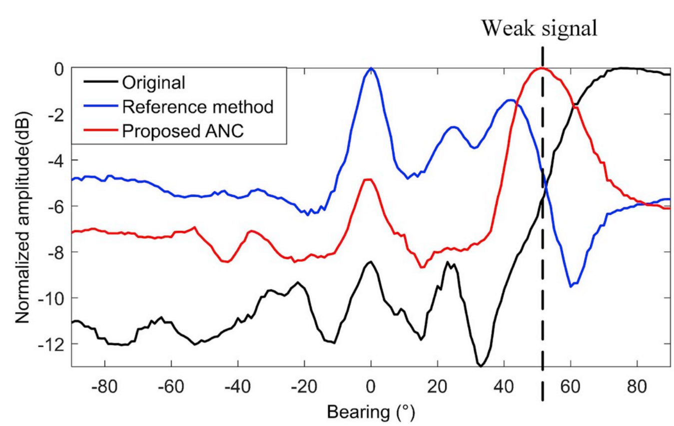

Fig. 12. Conventional array beamformer outputs for test case shown in Fig. 6. (Original: before AUV noise cancellation; Reference method: after AUV noise cancellation using the reference method; Proposed ANC: after AUV noise cancellation using the proposed adaptive noise canceller.)

ANC.

4.2. Computational complexity

The per sample computational complexity of the PFBLMS algorithm used in our ANC can be evaluated using Eq. (8.99) of reference Farhang-Boroujeny (2013), given as

$$C = (p+1)LP + \frac{3}{4}(p+1)\log_2\frac{(p+1)L}{2}. \tag{17}$$

The per sample computational complexity of the adaptive algorithm means the number of operations including multiplication and addition, required for processing one sample. According to Eq. (17), the per sample computational complexity of the PFBLMS algorithm used in the ANC is 50. As for the time-domain LMS-based algorithm with the filter length of 2048, 2048 multiplications are performed to compute the output (Haykin, 2002) per sample, and a further 2048 multiplications are required to update the tap weights. The per sample computational complexity of the time-domain LMS-based algorithms should be equal to or higher than 4096. Therefore, it can be concluded that the designed ANC is of much higher efficiency.

5. Conclusion

The design of an ANC to mitigate the impact of noise of an AUV on its towed array system is explored in detail in this paper. The experimental data used in this study showed that noise generated by an AUV can significantly interfere and thus limit the detection performance of its towed array system. The AUV noise spectrum mainly consisted of tonal components. The designed ANC employed the PBFLMS algorithm to obtain fast convergence speed and high efficiency, and took the beam output steered towards the AUV as the reference. The results indicated that the proposed ANC was able to recover a source signal embedded in a noise, which is 20 dB higher than the source signal. In terms of beamforming performance, it was observed that the reference method did not perform as good as the proposed ANC. The proposed ANC also has a shortcoming that its performance deteriorates for the signal direction of 60° onwards.

In our study, we injected a target signal numerically to test the performance of the ANC in recovering it in the presence of AUV noise. In the future, we plan to test the designed ANC with sources in water. Another area of interest is the study how the AUV speed impacts the noise characteristics and how the ANC can be adapted accordingly.

Author contribution section

Cheng Chi: Conceptualization, Methodology, Software, Validation, Formal analysis, Writing-Original Draft, Writing - Review & Editing. **Venugopalan Pallayil**: Conceptualization, Formal analysis, Investigation, Resources, Writing - Review & Editing, Supervision, Project administration, Funding acquisition. **Mandar Chitre**: Resources, Writing - Review & Editing, Supervision, Project administration, Funding acquisition.

Declaration of competing interest

The authors declare that they have no known competing financial interests or personal relationships that could have appeared to influence the work reported in this paper.

Appendix

In order to facilitate better understanding of the proposed ANC, Table 1 below summarizes the steps of the PFBLMS algorithm (Farhang-Boroujeny, 2013).

Table 1
Summary of the PFBLMS algorithm

Input:

Tap − weight vector, $\mathbf{w}_{F,l}(k),\ l = 0, 1, \ldots, P-1$,

Extended input vector, $\tilde{\mathbf{x}}_0(k) = [x(kL-M)\ x(kL-M+1)\ \ldots\ x(kL+L-1)]^{\mathrm{T}}$,

The past frequency domain vectors of input, $\mathbf{x}_{F,0}(k-l)$, *for* $k = 1, 2, \ldots, (P-1)p$,

Desired output vector, $\mathbf{d}(k) = [d(kL)\ d(kL+1)\ \ldots\ d(kL+L-1)]^{\mathrm{T}}$.

Output:

Filter output, $\mathbf{y}(k) = [y(kL)\ y(kL+1)\ \ldots\ y(kL+L-1)]^{\mathrm{T}}$,

Tap − weight vector update, $\mathbf{w}_{F,l}(k),\ l = 0, 1, \ldots, P-1$.

1 Filtering:

$\mathrm{x}_{F,0}(k) = \mathrm{FFT}(\tilde{\mathrm{x}}_0(k))$,

$$\mathbf{y}(k) = \text{the last L elements of IFFT}\left(\sum_{l=0}^{P-1} \mathbf{w}_{F,l}(k) \otimes \mathbf{x}_{F,0}(k-pl)\right)$$

2 Error estimation:

$\mathbf{e}(k) = \mathbf{d}(k) - \mathbf{y}(k)$

3 Step-normalization:

for $i = 0$ to M'

$\hat{\sigma}^2_{x_{F,0,i}}(k) = \beta\hat{\sigma}^2_{x_{F,0,i}}(k-1) + (1-\beta)|x_{F,0,i}(k)|^2$

$\mu_i(k) = \mu_0 / \hat{\sigma}^2_{x_{F,0,i}}(k)$

$\boldsymbol{\mu}(k) = [\mu_0(k)\ \mu_1(k)\ \ldots\mu_{M'-1}(k)\ ]^{\mathrm{T}}$

4 Tap-weight adaptation:

$$\mathrm{e}_F(k) = \mathrm{FFT}\left(\begin{bmatrix} \mathbf{0} \\ \mathbf{e}(k) \end{bmatrix}\right)$$

for $i = 0$ to $P-1$

$\mathbf{w}_{F,l}(k+1) = \mathbf{w}_{F,l}(k) + 2\boldsymbol{\mu}(k) \otimes \mathbf{x}^{*}_{F,0}(k-pl) \otimes \mathrm{e}_F(k)$

5 Tap-weight constraint:

for $i = 0$ to $P-1$

$$\mathbf{w}_{F,l}(k+1) = \left(\begin{bmatrix} \text{the first M elements of IFFT}(\mathbf{w}_{F,l}(k+1)) \\ \mathbf{0} \end{bmatrix}\right)$$

Notes.

◆ M: partition length; L: block length.$M' = M + L$.

◆ β is a constant close to, but smaller than 1.

◆ 0 denotes column zero vectors with appropriate length to extend vectors to the length M'.

◆ $\otimes$ denotes element-by-element multiplication of vectors; * denotes the conjugate operation.

◆ Step 5 is applicable only for the constrained PFBLMS algorithm.

References

Arveson, P.T., Vendittis, D.J., 2000. Radiated noise characteristics of a modern cargo ship. J. Acoust. Soc. Am. 107, 118–129.

Candy, J.V., Sullivan, E.J., 2005. Cancelling tow ship noise using an adaptive model-based approach. In: Proceedings of the IEEE/OES Eighth Working Conference on Current Measurement Technology. Southampton, UK.

Cederholm, A., Jönsson, M., 2008. Self-noise Cancellation Methods Applied to Acoustic Underwater Sensors. Technical report (No. FOI-R-2573-SE).

Chotiros, N., Pallayil, V., 2013. Seabed characterization using acoustic communication signals on an autonomous underwater vehicle with a thin-line towed array. IEEE J. Ocean. Eng. 38, 410–418.

Cheng, C., Pallayil, V., 2017. Noise cancellation for an autonomous undwater vehicle-twoed thin line array through recursive adaptive filtering. J. Acoust. Soc. Am. 141, 3925.

Farhang-Boroujeny, B., 2013. Adaptive Filters: Theory and Applications. John Wiley & Sons, pp. 251–288 (chapter 8).

Ferri, G., Munafò, A., LePage, K., 2018. An autonomous underwater vehicle data-driven control strategy for target tracking. IEEE J. Ocean. Eng. 43, 323–343.

Glegg, S.A.L., Olivieri, M.P., Coulson, R.K., Smith, S.M., 2001. A passive sonar system based on an autonomous underwater vehicle. IEEE J. Ocean. Eng. 26, 700–710.

Griffiths, G., Enoch, P., Milard, N.W., 2001. On the radiated noise of the autosub autonomous underwater vehicle. ICES (Int. Counc. Explor. Sea) J. Mar. Sci. 58, 1195–1200.

Harrison, W.A., Lim, J.S., Singer, E., 1986. A new application of adaptive noise cancellation. IEEE Trans. Acoust. Speech Signal Process. 34, 21–27.

Haykin, S.O., 2002. Adaptive Filters Theory, fourth ed. Pearson Higher Ed, pp. 344–355.

Hodges, R.P., 2011. Underwater Acoustics: Analysis, Design and Performance of Sonar. John Wiley & Sons, pp. 183–192.

Holmes, J.D., Carey, W.M., Lynch, J.F., Newhall, A.E., Kukulya, A., 2005. An autonomous underwater vehicle towed array for ocean acoustic measurements and inversions. In: Proceedings of Oceans. Brest, France, pp. 1–4, 2005.

Holmes, J.D., Carey, W.M., Lynch, J.F., 2006. Results from an autonomous underwater vehicle towed hydrophone array experiment in Nantucket Sound. J. Acoust. Soc. Am. 120, EL15–21.

Holmes, J.D., Carey, W.M., Lynch, J.F., 2010. An overview of unmanned underwater vehicle noise in the low to mid frequencies bands. Proc. Meet. Acoust. 9, 1–17.

Kuperman, W.A., Werby, M.F., Gilbert, K.E., 1985. Towed array response to ship noise: a near-field propagation. In: Adaptive Methods in Underwater Acoustics. Springer Science & Business Media, pp. 71–80.

Li, Q., 2012. Digital Sonar Design in Underwater Acoustics: Principles and Applications. Springer Science & Business Media, pp. 540–542.

Maguer, A., Dymond, R., Mazzi, M., Biagini, S., Fioravanti, S., Guerrini, P., 2008. SLITA: a new towed array for AUV applications. In: Proceedings of Acoustics 08 Paris, pp. 323–328.

Munafò, A., Ferri, G., LePage, K., Goldhahn, R., 2017. AUV active perception: exploiting the water column. In: Proceedings of OCEANS. Aberdeen, UK, 2017.

Newhall, A.E., Lin, Y., Grothues, T.M., Lynch, J.F., Gawarkiewicz, G.G., 2017. A method of observing acoustic scattering and absorption by fish schools using autonomous underwater vehicles. IEEE J. Ocean. Eng. 42, 29–36.

Pallayil, V., Chitre, M., Deshpande, P.D., 2007. A digital thin line towed array for small autonomous underwater platform. In: Proceedings of OCEANS, pp. 1–9, 2007, Vancouver, Canada.

Pallayil, V., Muttuthupara, S., Chitre, M., Govind, K., 2009. Characterization of a digital thin line towed array experimental assessment of vibration levels and tow shape. In: Underwater Acoustic Measurements. Nafplion, Greece, pp. 21–26, 2009.

Robert, M.K., Beerens, S.P., 2002. Adaptive beamforming algorithms for tow ship noise canceling. In: Proceedings of Undersea Defence Technology Europe 2002. La Spezia, Italy.

Sullivan, E.J., Candy, J.V., 2005. Enhanced processing for a towed array using an optimal noise cancelling approach. In: Proceeding of OCEANS, 2005, Washington DC, USA.

Van Trees, H.L., 2004. Optimum Array Processing: Part IV of Detection, Estimation, and Modulation Theory. John Wiley & Sons, pp. 64–66.

Widrow, B., Glover, J.R., McCool, J.M., Kaunitz, J., Williams, C.S., Hearn, R.H., Zeidler, J.R., Dong Jr., E., Goodlin, R.C., 1975. Adaptive noise cancelling: principles and applications. Proc. IEEE 63, 1692–1716.

Zimmerman, R., D'Spain, G.L., Chadwell, C.D., 2005. Decreasing the radiated acoustic and vibration noise of a mid-size AUV. IEEE J. Ocean. Eng. 30, 179–187.